Adaptive Design Specifications and Coarsely-Discretized EM Models for Rapid Optimization of Microwave Structures

Slawomir Koziel

Engineering Optimization & Modeling Center, School of Science and Engineering
Reykjavik University, 101 Reykjavik, Iceland
koziel@ru.is

Abstract **─** A simple and efficient procedure for EM-simulation-driven design optimization of microwave devices is discussed. Our approach exploits recently introduced adaptively adjusted design specifications technique that shifts the optimization burden into a relaxed-accuracy and computationally cheap (low-fidelity) model of the structure under consideration, evaluated using the same EM solver as the original (high-fidelity) model but with coarse discretization. The unavoidable misalignment between the low- and high-fidelity models is accounted for by suitable adjustments of the design specifications. The presented method is simple to implement and allows rapid design improvement as demonstrated through examples.

Index Terms **─** Adaptive design specifications, computer-aided design (CAD), electromagnetic simulation, simulation-driven design.

I. INTRODUCTION

Simulation-driven design and design optimization is ubiquitous in contemporary microwave engineering. For many classes of microwave structures no systematic design procedures are available so that EM-based design becomes the only option. Examples include ultrawideband (UWB) antennas [1], dielectric resonator antennas [2] and substrate integrated circuits [3]. On the other hand, increasing complexity of microwave devices and the demand for high accuracy make the direct optimization involving numerous electromagnetic (EM) simulations impractical because of the computational cost of such a process. Co-simulation [4-6] is only a partial solution because the circuit models with embedded EM components are still directly optimized.

A cost-efficient design of microwave structures exploiting EM solvers can be realized using surrogate-based optimization (SBO) [7, 8]. In SBO, the direct optimization of the CPU-intensive EM-evaluated structure of interest (high-fidelity model) is replaced by iterative updating and re-optimization of its computationally cheap representation, the surrogate. The successful SBO approaches in microwave area are space mapping (SM) [9-16] and various forms of tuning [17, 18] as well as combinations of both [19, 20]. Other SBO methods used in microwave engineering include manifold mapping [28] as well as techniques exploiting variable-fidelity EM simulations [29, 30]. Space mapping builds the surrogate using a physically-based low-fidelity model, typically an equivalent circuit. Tuning approaches are based on embedding circuit-theory-based tuning elements into the structure of interest using properly located internal ports [18]. Both approaches can be very efficient and yield satisfactory designs after a few full-wave EM simulations of the structures under consideration [9, 18].

Unfortunately, implementation of both SM and tuning may not be straightforward. In particular, modification of the structure being optimized and engineering experience may be required (tuning), additional mapping and more or less complicated interaction between various auxiliary models is necessary (SM). In order to take advantage of space mapping, the low-fidelity model should be computationally much cheaper

Submitted On: January 21, 2011
Accepted On: October 18, 2011

than the high-fidelity model, therefore, equivalent-circuit models are preferred [9]. Reliable equivalent-circuit models, however, may be difficult to develop for certain types of microwave devices (e.g., antennas). Also, an extra simulator must be involved in the process and linked to the optimization algorithm. Moreover, space mapping performance heavily depends on the selection of the SM transformations used to construct the surrogate. On the other hand, tuning cannot be directly applied to radiating structures.

In this paper, an efficient technique for simulation-driven design of EM-simulated structures is discussed that is based on the SBO principle, coarsely-discretized EM low-fidelity models, and adaptive adjustment of the design specifications [21]. Original design specifications are modified to take into account the difference between the high-fidelity and low-fidelity model responses at the current design. The low-fidelity model is then optimized with respect to the modified specifications to produce a new design that—assuming sufficient quality of the low-fidelity model—gives a good prediction of the optimal high-fidelity model design with respect to the original specifications. The above assumption is typically satisfied for coarsely-discretized EM models. The presented method is simple to implement, and, as demonstrated through examples, it is able to yield a satisfactory design after a few high-fidelity EM simulations of the structure under considerations.

II. SIMULATION-DRIVEN DESIGN METHODOLOGY

In this section, we formulate the optimization problem (Section II. A), describe the concept of adaptively adjusted design specifications technique (Section II. B), as well as comment upon the use of coarse-discretization EM simulations as the low-fidelity model guiding the optimization process (Section II. C).

A. Design optimization problem

Let $\boldsymbol{R}_f(\boldsymbol{x})$ and $\boldsymbol{R}_c(\boldsymbol{x})$ denote the response vectors of a high- and low-fidelity models of the microwave structure of interest at the design vector x. For example, $\boldsymbol{R}_f(\boldsymbol{x})$ may consist of the values of $|S_{21}|$ evaluated at a set of frequencies. The high-fidelity model is evaluated using CPU-intensive electromagnetic simulation. The low-fidelity model is a relaxed-accuracy and computationally cheap representation of $\boldsymbol{R}_f$. In particular, $\boldsymbol{R}_c$ may be evaluated using the same solver as $\boldsymbol{R}_f$ but with coarser mesh.

We want to optimize the high-fidelity model with respect to a given set of design specifications. Figure 1(a) shows the high- and low-fidelity model responses at the optimal design of $\boldsymbol{R}_c$, corresponding to the microstrip bandstop filter [21] used here as an illustration example; design specifications are indicated using horizontal lines.

B. Optimization through adaptively adjusted design specifications

The optimization procedure based on adaptively adjusted design specifications, originally introduced in [21], consists of the following two simple steps that can be iterated if necessary:

1. Modify the original design specifications in order to take into account the difference between the responses of $\boldsymbol{R}_f$ and $\boldsymbol{R}_c$ at their characteristic points.
2. Obtain a new design by optimizing the low-fidelity model with respect to the modified specifications.

Characteristic points of the responses should correspond to the design specification levels. They should also include local maxima/minima of the respective responses at which the specifications may not be satisfied. Figure 1(b) shows characteristic points of $\boldsymbol{R}_f$ and $\boldsymbol{R}_c$ for our bandstop filter example. The points correspond to –3 dB and –30 dB levels as well to the local maxima of the responses. As one can observe in Fig. 1(b), the selection of points is rather straightforward.

In the first step of the optimization procedure, the design specifications are modified so that the level of satisfying/violating the modified specifications by the low-fidelity model response corresponds to the satisfaction/violation levels of the original specifications by the high-fidelity model response. More specifically, for each edge of the specification line, the edge frequency is shifted by the difference of the frequencies of the corresponding characteristic points, e.g., the left edge of the specification line of –30 dB is moved to the right by about 0.7 GHz, which is equal to the length of the line connecting the corresponding characteristic points in Fig. 1(b). Similarly, the specification levels are shifted by the difference between the local maxima/minima values for the respective points, e.g., the –30 dB level is shifted down by about 8.5 dB because of the difference of the local maxima of the corresponding characteristic points of $\boldsymbol{R}_f$ and $\boldsymbol{R}_c$. Modified design specifications are shown in Fig. 1(c).

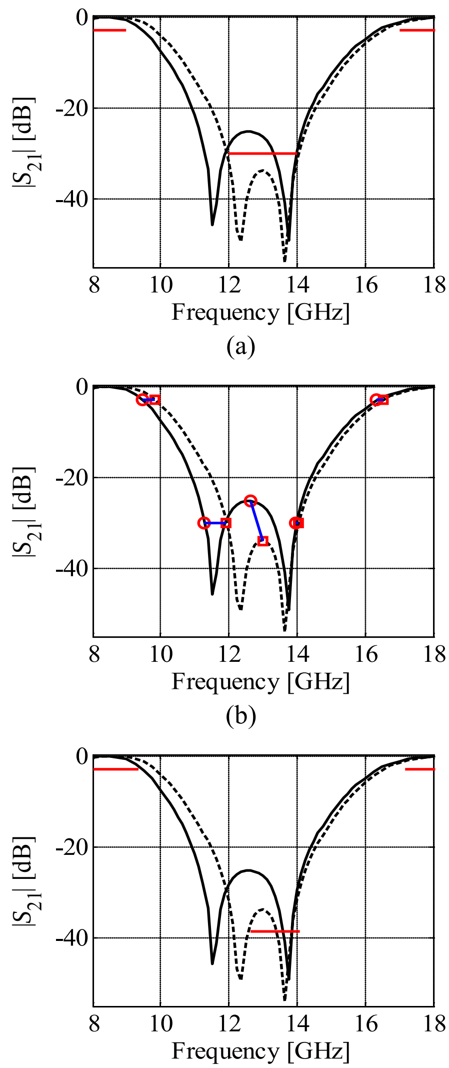

Fig. 1. Bandstop filter example (responses of $\boldsymbol{R}_f$ and $\boldsymbol{R}_c$ are denoted using solid and dashed line, respectively) [21]: (a) responses at the initial design (low-fidelity model optimum) as well as the original design specifications, (b) characteristic points of the responses corresponding to the specification levels (here, -3 dB and -30 dB) and to the local maxima, (c) responses at the initial design as well as the modified design specifications.

The low-fidelity model is subsequently optimized with respect to the modified specifications and the new design obtained this way is treated as an approximated solution to the original design problem (i.e., optimization of the high-fidelity model with respect to the original specifications). Steps 1 and 2 can be repeated if necessary. As demonstrated in Section III, substantial design improvement is typically observed after the first iteration, however, additional iterations may bring further enhancement. In practice, the algorithm is terminated once the current iteration does not bring further improvement of the high-fidelity model design.

Figure 2 shows the flow diagram of the optimization procedure. It should be emphasized, that unlike in case of other simulation-driven techniques popular in microwave engineering (particularly space mapping [9]), the low-fidelity model is not modified or corrected in any way. The discrepancy between the models is “absorbed” by means of modifying the design specifications.

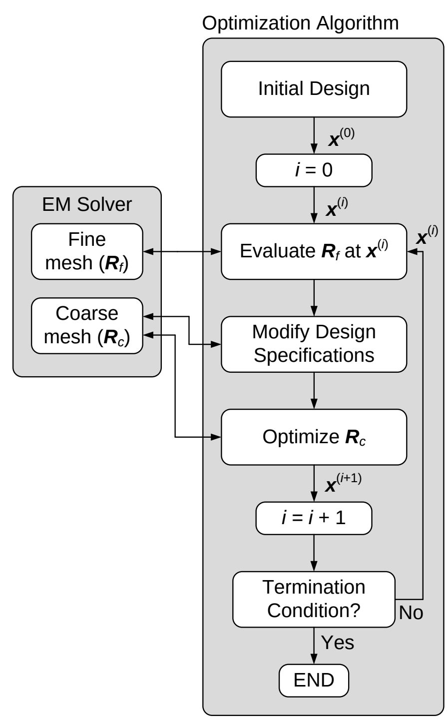

Fig. 2. A flow diagram of the optimization procedure exploiting adaptively adjusted design specifications and coarse-discretization EM models.

The operation of the adaptively adjusted design specifications technique can probably be best explained using the example. Figure 3 illustrates an iteration of the procedure used for design of a CBCPW-to-SIW transition [31]. One can observe that the absolute matching between the low- and high-fidelity models is not as important as the shape similarity.

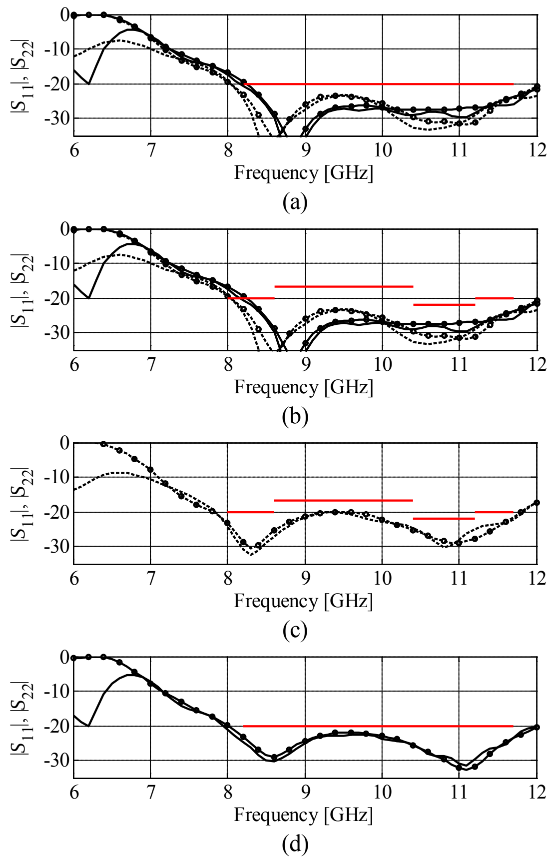

Fig. 3: Adaptively adjusted design specification technique applied to optimize CBCPW-to-SIW transitions. High- and low-fidelity model response denoted as solid and dashed lines, respectively. $|S_{22}|$ distinguished from $|S_{11}|$ using circles. Design specifications denoted by thick horizontal lines. (a) High- and low-fidelity model responses at the beginning of the iteration as well as original design specifications; (b) high- and low-fidelity model responses and modified design specifications that reflect the differences between the responses; (c) low-fidelity model optimized to meet the modified specifications; (d) high-fidelity model at the low-fidelity model optimum shown versus original specifications. Thick horizontal lines indicate the design specifications.

It should be stressed that the low-fidelity model is not modified in any way, that is, no changes are applied to it in order to align it with the high-fidelity model. The discrepancy between the high- and low-fidelity model responses is accounted for by modifying the design specifications.

C. Coarsely-discretized EM-simulation models

While in general, the low-fidelity model can be any physically-based model that is available (e.g., equivalent circuit [9]), the coarse-discretization EM models are used here. This has several advantages: (i) coarse-discretization models using the same EM solvers as corresponding fine models are typically more accurate than any other models of a given structure (e.g., equivalent circuits), (ii) optimization procedure is easy to implement because it exploits one software package (in the case of circuit-based low-fidelity models, an extra simulator is necessary which complicates the algorithm implementation because interaction the simulators has to be realized), (iii) coarse-discretization EM model typically provides better initial design than any other conceivable low-fidelity model type, (iv) coarse-discretization model is available for any microwave structure; in particular, the optimization can performed for devices where finding equivalent circuit model may be problematic (e.g., antennas).

One of the possible problems is that coarse-discretization EM models are relatively expensive so that minimizing the number of low-fidelity model evaluations is crucial in reducing the computational cost of the optimization process. It should be emphasized, however, that the procedure described here is quite efficient with this respect. In particular, it does not have a parameter extraction step—typical for space mapping approaches [12]—that normally requires consumes a substantial number of low-fidelity model evaluations.

D. Practical issues

The adaptively adjusted design specifications technique is very simple to implement and quite efficient as demonstrated in Section III. It should be emphasized, however, that the quality of the low-fidelity model is essential for the performance of this design procedure. More specifically, it is necessary that the high- and low-fidelity models are similar in shape (as functions of frequency) so that modification of the design specifications can be a relevant tool reflecting their misalignment. This requires that the discretization density for the low-fidelity model is sufficient; otherwise, the method may fail to find a satisfactory design. In practice, a parametric study of the mesh density and visual comparison of the high- and low-fidelity model responses are necessary to select the meshing parameters for the latter.

III. EXAMPLES

A. Double annular ring antenna [22]

Consider the stacked probe-fed printed annular ring antenna [22] shown in Fig. 4. The antenna is printed on a printed circuit board (PCB) with electrical permittivity $\varepsilon_{r1} = 2.2$, and height $d_1 = 6.096$ mm for the lower substrate, and $\varepsilon_{r2} = 1.07$, $d_2 = 8.0$ mm for the upper substrate. The radius of the feed pin is $r_0 = 0.325$ mm. The design parameters are $\boldsymbol{x} = [a_1\ a_2\ b_1\ b_2\ \rho_1]^T$.

The fine model is evaluated using FEKO [23]. Its response is the modulus of the reflection coefficient, $|S_{11}|$, evaluated over the frequency band 1.75 GHz to 2.15 GHz. The number of meshes for $\boldsymbol{R}_f$ is 1480 and its evaluation time is 2 hours and 5 minutes. The design specifications are $|S_{11}| \leq -10$ dB for 1.75 GHz $\leq \omega \leq$ 2.15 GHz. The coarse model $\boldsymbol{R}_c$ is also simulated in FEKO. The number of meshes for $\boldsymbol{R}_c$ is 300. The coarse model evaluation time is 6 minutes and 30 seconds. Initial design $\boldsymbol{x}^{(0)} = [10\ 8\ 30\ 30\ 20]^T$ mm.

Optimization of the antenna was performed using the adaptively adjusted design specifications technique described in Section II. Figure 5 shows the fine and coarse model responses at the initial design (minimax specification error +6.0 dB), as well as the fine model response at the final design $\boldsymbol{x}^{(2)} = [10.81\ 5.75\ 28.5\ 32.25\ 19.5]^T$ mm (specification error is –0.2 dB) obtained after two iterations of our procedure. The total number of evaluations of the coarse model in the optimization process is 87. Table 1 shows the computational cost of the optimization: the total optimization time corresponds to only 6.5 evaluations of the fine model. For comparison purposes, the direct optimization of the fine model using Matlab's *fminimax* routine was performed using $\boldsymbol{x}^{(0)}$ as a starting point. A slightly better design was obtained (with the specification error of –0.5 dB) at much higher cost of 55 fine model evaluations (almost 115 hours of CPU time).

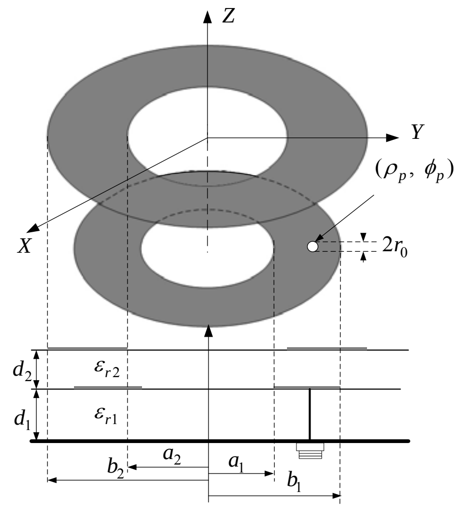

Fig. 4. Geometry of a stacked probe-fed printed double annular ring antenna [22].

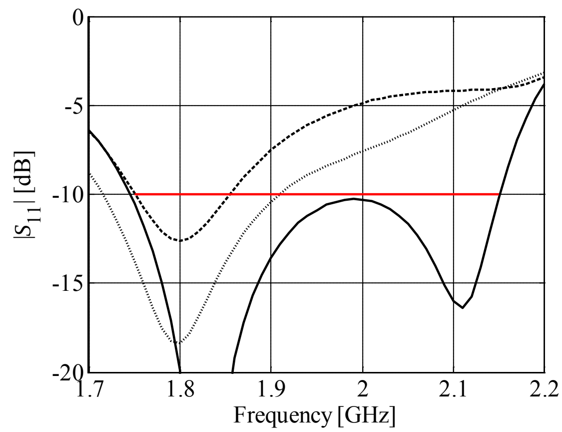

Fig. 5. Double annular ring antenna: High- (- - -) and low-fidelity (· · ·) model responses at the initial design $\boldsymbol{x}^{(0)}$, and the high-fidelity model response at the final design found by the adaptive design specifications technique (—).

Table 1: Computational cost of optimizing the double annular ring antenna

Algorithm Component	Number of Model Evaluations	Optimization Time	
		Absolute [min]	Relative[#]
Evaluation of $\boldsymbol{R}_c$	87	565	4.5
Evaluation of $\boldsymbol{R}_f$	2[*]	250	2.0
Total optimization time	N/A	815	6.5

[*] Excluded evaluation of the fine model at the initial design
[#] Number of high-fidelity model evaluations

B. Miniature dual-mode bandpass microstrip filter [24]

Consider the miniature dual-mode bandpass filter [24] shown in Fig. 6. The design parameters are $\boldsymbol{x} = [L\ s\ p\ g]^T$; W = 1 mm, W_c = 0.5 mm. Both the fine and coarse models are evaluated in FEKO [23]. The total mesh number for the fine model is 646 (evaluation time 20 min), the total mesh number for the coarse model is 68 (evaluation time 26 seconds). The design specifications are $|S_{21}| \geq -1$ dB for 2.35 GHz $\leq \omega \leq$ 2.45 GHz, $|S_{21}| \leq -20$ dB for 1.6 GHz $\leq \omega \leq$ 2.2 GHz and for 2.6 GHz $\leq \omega \leq$ 3.2 GHz. The initial design is $\boldsymbol{x}^{(0)} = [12.0\ 2.0\ 2.0\ 0.2]^T$ mm.

The adaptively adjusted design specifications technique of Section 2 was used to optimize the filter. Figure 7 shows the fine model and coarse model responses at the initial design (minimax specification error +19.6 dB), as well as the fine model response at the final design $\boldsymbol{x}^{(3)} = [12.65\ 1.99\ 1.38\ 0.145]^T$ mm (specification error is –0.2 dB) obtained after three iterations of the optimization procedure. The total number of evaluations of the coarse model in the optimization process is 137. The total cost of the design process corresponds to only 5.9 evaluations of the fine model (Table 2). For comparison purposes, the direct optimization of the fine model using Matlab's *fminimax* routine was performed using $\boldsymbol{x}^{(0)}$ as a starting point. This direct optimization failed to find a design satisfying the specifications (algorithm terminated after 120 function evaluations, i.e., 40 hours of CPU time, best design found corresponds to +5.2 dB). Optimization of the fine model using pattern search algorithm [25] resulted in the satisfactory design (specification error –0.4 dB); however, the cost was quite high (97 fine model evaluations, over 32 hours of CPU time).

C. UWB monopole antenna

The monopole is on a 0.508 mm thick Rogers RO3203 substrate. Design variables are $\boldsymbol{x} = [h_0\ w_0\ a_0\ s_0\ h_1\ w_1\ l_{gnd}\ w_s]^T$ (Fig. 8). Other parameters: l_s = 25, w_m = 1.25, h_p =0.75 (all in mm). The microstrip input of the monopole is fed through an edge mount SMA connector [26] having a hex nut. The ground of the monopole has a profiled edge. Both high- and low-fidelity models are evaluated using the time-domain solver of CST Microwave Studio [27]. Simulation time of $\boldsymbol{R}_c$ (152,640 mesh cells) is 2 min, and that of $\boldsymbol{R}_f$ (1,151,334 mesh cells) is 45 min (both at the initial design). The design specifications for reflection are $|S_{11}| \leq -10$ dB for 3.1 GHz to 10.6 GHz. Additionally, the radiation pattern of the monopole is to be omnidirectional in the *XOY* plane.

Initial design $\boldsymbol{x}^{(0)} = [18\ 12\ 2\ 0\ 5\ 1\ 15\ 40]^T$ mm. Optimization performed using the adaptively adjusted design specifications technique yields the final design $\boldsymbol{x}^{(3)} = [18.27\ 19.41\ 2.02\ 1.34\ 1.95\ 5.83\ 15.74\ 35.75]^T$ mm ($|S_{11}| < -14.5$ dB in the frequency band of interest) obtained after three iterations of our procedure. Figure 9 shows reflection responses of the high- and low-fidelity models at the initial design as well as the $\boldsymbol{R}_f$ response at the final design. The far-field response of the final design is shown in Fig. 10. The total number of evaluations of $\boldsymbol{R}_c$ in the optimization process is 252. Table 3 shows the computational cost of the optimization: the total optimization time corresponds to about 14 evaluations of the high-fidelity model.

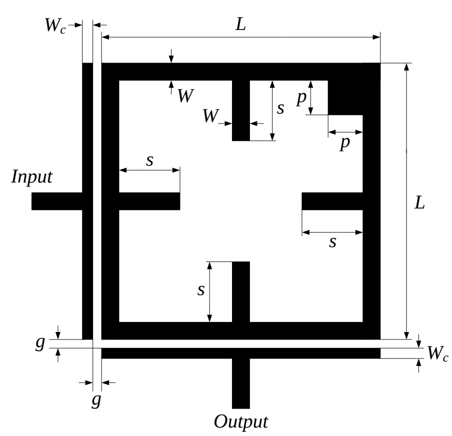

Fig. 6. Miniature dual-mode bandpass filter: geometry [24].

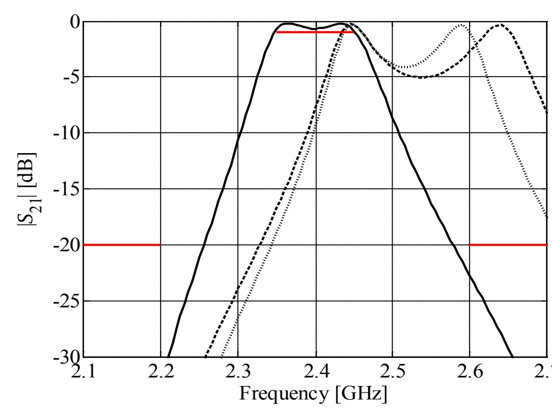

Fig. 7. Miniature dual-mode bandpass filter: High- (- - -) and low-fidelity (· · ·) model responses at the initial design $\boldsymbol{x}^{(0)}$, and the high-fidelity model response at the final design found by the adaptive design specifications technique (—).

Table 2: Computational cost of optimizing the miniature dual-mode bandpass filter

Algorithm Component	Number of Model Evaluations	Optimization Time	
		Absolute [min]	Relative[#]
Evaluation of $\boldsymbol{R}_c$	137	59	2.9
Evaluation of $\boldsymbol{R}_f$	3[*]	60	3.0
Total optimization time	N/A	119	5.9

[*] Excluded evaluation of the fine model at the initial design
[#] Number of high-fidelity model evaluations

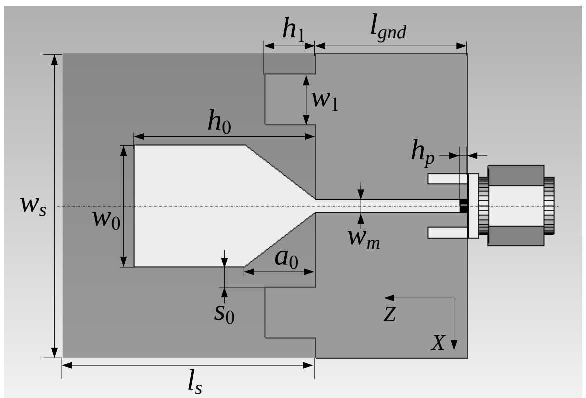

Fig. 8. UWB monopole: top view, substrate shown transparent. *H*-symmetry wall is shown with the dash-dot line.

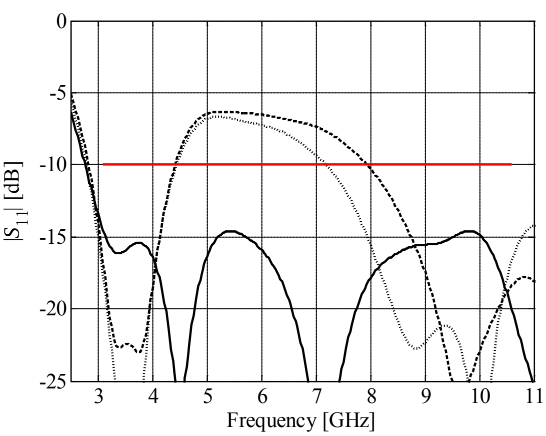

Fig. 9. UWB monopole antenna: High- (dashed line) and low-fidelity (dotted line) model responses at the initial design $\boldsymbol{x}^{(0)}$, and the high-fidelity model response at the final design found by the adaptive design specifications technique (solid line).

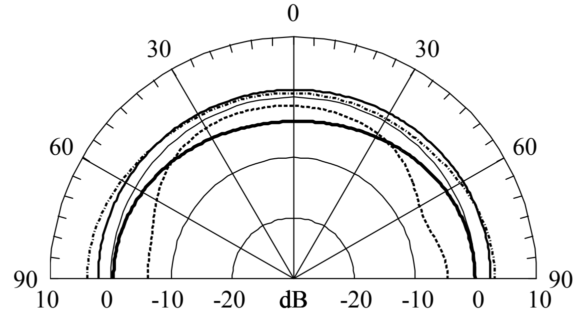

Fig. 10. Realized gain (x-pol.) of the UWB monopole: pattern cut in XOY plane at 3 GHz (—), 5 GHz (▬), 7 GHz (- · · · -), and 9 GHz (- - -). 90^0 on the left, 0^0, and 90^0 on the right are for *Y*, *X*, and –*Y* directions, respectively.

Table 3: Computational cost of optimizing the UWB monopole antenna

Algorithm Component	Number of Model Evaluations	Optimization Time	
		Absolute [hours]	Relative[#]
Evaluation of $\boldsymbol{R}_c$	252	8.4	11.2
Evaluation of $\boldsymbol{R}_f$	3[*]	2.3	3.0
Total optimization time	N/A	10.7	14.2

[*] Excluded evaluation of the fine model at the initial design
[#] Number of high-fidelity model evaluations

IV. CONCLUSION

An efficient procedure for design optimization of EM-simulated microwave devices is discussed. The presented approach exploits a computationally cheap model of the structure under consideration, evaluated using the same electromagnetic solver but with coarse discretization. The misalignment between the low- and high-fidelity EM models is absorbed by suitable adjustments of the design specifications. The performance of the presented technique is demonstrated through the design of the double annular ring antenna, the microstrip bandpass filter, and the UWB monopole antenna. Satisfactory designs are obtained at the computational cost corresponding to a few high-fidelity EM simulations of the respective structures.

ACKNOWLEDGMENT

This work was supported in part by the Icelandic Centre for Research (RANNIS) Grant 110034021.

REFERENCES

[1] H. Schantz, *The Art and Science of Ultrawideband Antennas*, Artech House, 2005.

[2] A. Petosa, *Dielectric Resonator Antenna Handbook*, Artech House, 2007.

[3] K. Wu, "Substrate Integrated Circuits (SiCs) – A New Paradigm for Future Ghz and Thz Electronic and Photonic Systems," *IEEE Circuits and Systems Society Newsletter,* vol. 3, no. 2, Apr. 2009.

[4] R. V. Snyder, "Practical Aspects of Microwave Filter Development," *IEEE Microwave Magazine*, vol. 8, no. 2, pp. 42-54, Apr. 2007.

[5] S. Shin and S. Kanamaluru, "Diplexer Design using EM and Circuit Simulation Techniques," *IEEE Microwave Magazine*, vol. 8, no. 2, pp. 77-82, Apr. 2007.

[6] V. Rizzoli, A. Costanzo, D. Masotti, and P. Spadoni, "Circuit-Level Nonlinear/Electromagnetic Co-Simulation of an Entire Microwave Link," *IEEE MTT-S Int. Microwave Symp. Dig.*, Long Beach, CA, pp. 813-816, June 2005.

[7] N. V. Queipo, R. T. Haftka, W. Shyy, T. Goel, R. Vaidynathan, and P. K. Tucker, "Surrogate-Based Analysis and Optimization," *Progress in Aerospace Sciences*, vol. 41, no. 1, pp. 1-28, Jan. 2005.

[8] A. I. J. Forrester and A. J. Keane, "Recent Advances in Surrogate-Based Optimization," *Prog. in Aerospace Sciences*, vol. 45, no. 1-3, pp. 50-79, Jan.-April 2009.

[9] J. W. Bandler, Q. S. Cheng, S. A. Dakroury, A. S. Mohamed, M. H. Bakr, K. Madsen, and J. Søndergaard, "Space Mapping: The State of the Art," *IEEE Trans. Microwave Theory Tech.*, vol. 52, no. 1, pp. 337-361, Jan. 2004.

[10] D. Echeverria and P. W. Hemker, "Space Mapping and Defect Correction," *CMAM The International Mathematical Journal Computational Methods in Applied Mathematics,* vol. 5, no. 2, pp. 107-136, 2005.

[11] S. Amari, C. LeDrew, and W. Menzel, "Space-Mapping Optimization of Planar Coupled-Resonator Microwave Filters," *IEEE Trans. Microwave Theory Tech.*, vol. 54, no. 5, pp. 2153-2159, May 2006.

[12] S. Koziel, Q. S. Cheng, and J. W. Bandler, "Space Mapping," *IEEE Microwave Magazine*, vol. 9, no. 6, pp. 105-122, Dec. 2008.

[13] G. Crevecoeur, P. Sergeant, L. Dupre, and R. Van de Walle, "Two-Level Response and Parameter Mapping Optimization for Magnetic Shielding," *IEEE Trans. on Magnetics*, vol. 44, no. 2, pp. 301-308, Feb. 2008.

[14] M. F. Pantoja, P. Meincke, and A. R. Bretones, "A Hybrid Genetic-Algorithm Space-Mapping Tool for the Optimization of Antennas," *IEEE Trans. Antennas and Propagation*, vol. 55, no. 3, Part 1, pp. 777-781, March 2007.

[15] T. V. Tran, S. Brisset, and P. Brochet, "A New Efficient Method for Global Multilevel Optimization Combining Branch-and-Bound and Space Mapping," *IEEE Trans. Magn.*, vol. 45, no. 3, pp. 1590-1593, 2009.

[16] J. Quyang, F. Yang, H. Zhou, Z. Nie, and Z. Zhao, "Conformal Antenna Optimization with Space Mapping," *J. of Electromagn. Waves and Appl.*, vol. 24, no. 2-3, pp. 251-260, 2010.

[17] D. Swanson and G. Macchiarella, "Microwave Filter Design by Synthesis and Optimization," *IEEE Microwave Magazine*, vol. 8, no. 2, pp. 55-69, Apr. 2007.

[18] J. C. Rautio, "Perfectly Calibrated Internal Ports in EM Analysis of Planar Circuits," *IEEE MTT-S Int. Microwave Symp. Dig.*, Atlanta, GA, pp. 1373-1376, June 2008.

[19] S. Koziel, J. Meng, J. W. Bandler, M. H. Bakr, and Q. S. Cheng, "Accelerated Microwave Design Optimization with Tuning Space Mapping," *IEEE Trans. Microwave Theory and Tech.*, vol. 57, no. 2, pp. 383-394, 2009.

[20] Q. S. Cheng, J. W. Bandler, and S. Koziel, "Space Mapping Design Framework Exploiting Tuning Elements," *IEEE Trans. Microwave Theory and Tech.*, vol. 58, no. 1, pp. 136-144, 2010.

[21] S. Koziel, "Efficient Optimization of Microwave Structures through Design Specifications Adaptation," *IEEE Int. Symp. Antennas Prop.*, Toronto, Canada, 2010.

[22] D. M. Kokotoff, J. T. Aberle, and R. B. Waterhouse, "Rigorous Analysis of Probe-Fed Printed Annular Ring Antennas," *IEEE Trans. Antennas Propagat*, vol. 47, no. 2, pp. 384-388, Feb. 1999.

[23] FEKO, Suite 5.3, EM Software & Systems-S.A. (Pty) Ltd, 32 Techno Lane, Technopark, Stellenbosch, 7600, South Africa, 2008.

[24] Y. F. Lin, C. H. Chen, K. Y. Chen, H. M. Chen, and K. L. Wong, "A Miniature Dual-Mode Bandpass Filter using Al_2O_3 Substrate," *IEEE Microw. Wireless Compon. Lett.*, vol. 17, no. 8, pp. 580-582, Aug. 2007.

[25] T. G. Kolda, R. M. Lewis, and V. Torczon, "Optimization by Direct Search: New Perspectives on Some Classical and Modern Methods," *SIAM Review*, vol. 45, no. 3, pp. 385-482, 2003.

[26] SMA Edge Mount P.C. Board Receptacles, Catalog, Applied Engineering Products, New Haven, CT, USA.

[27] CST Microwave Studio, ver. 2009, CST AG, Bad Nauheimer Str. 19, D-64289 Darmstadt, Germany, 2009.

[28] D. Echeverria and P.W. Hemker, "Space mapping and defect correction," *CMAM Int. Mathematical Journal Computational Methods in Applied Mathematics,* vol. 5, pp. 107-136, 2005.

[29] S. Koziel, "Multi-Fidelity Optimization of Microwave Structures using Response Surface Approximation and Space Mapping," *Applied Computational Electromagnetic Society (ACES) Journal*, vol. 24, no. 6, pp. 600–608, December 2009.

[30] S. Koziel, "Computationally Efficient Multi-fidelity Multi-Grid Design Optimization of Microwave Structures," *Applied Computational Electromagnetic Society (ACES) Journal*, vol. 25, no. 7, pp. 578–586, July 2010.

[31] D. Deslandes and K. Wu, "Analysis and Design of Current Probe Transition from Grounded Coplanar to Substrate Integrated Rectangular Waveguides," *IEEE Trans. Microw. Theory Tech.*, vol. 53, no. 8, Aug. 2005, pp. 2487-2494.

Slawomir Koziel received the M.Sc. and Ph.D. degrees in Electronic Engineering from Gdansk University of Technology, Poland, in 1995 and 2000, respectively. He also received the M.Sc. degrees in Theoretical Physics and in Mathematics, in 2000 and 2002, respectively, as well as the Ph.D. in Mathematics in 2003, from the University of Gdansk, Poland. He is currently an Associate Professor with the School of Science and Engineering, Reykjavik University, Iceland. His research interests include CAD and modeling of microwave circuits, surrogate-based optimization, space mapping, circuit theory, analog signal processing, evolutionary computation and numerical analysis.